MODEY, PAUL. MS. Mechanical Evaluation of Various Geometrical Designs In Additive Manufacturing For Future Knee Brace Harness. (2024)
Directed by Dr. Dennis LaJeunesse. 49 pp.

Additive manufacturing, commonly known as 3D printing, revolutionizes the realization of computer-aided designs (CAD) by layer-by-layer printing of prototypes or objects, emulating traditional modeling techniques. Also, according to ASTM standards, additively manufactured prototypes using plastics must undergo the tensile strength testing using the ASTM D638 - 14 Standard Test Method for Tensile Properties of Plastics. The objective was to fabricate and analyze the effects of different geometries on the mechanical properties of the produced meshes. I also determined the differences in mechanical properties when it comes to materials used in printing. Three different geometries (simple grid with holes, hexagonal grid, and zig-zag patterns) were printed using five different photopolymer resin types, and their tensile modulus (Young's Modulus, YM, of Elasticity) and tensile strength were examined using a mechanical strength analyzer. Simple grid with holes (Mean YM ≈ 1.255 MPa) showed higher strength whilst the hexagonal grid pattern showed the least strength mechanically (Mean YM ≈ 0.346 MPa) Translucent photopolymer resin with average YM of 0.0.231 MPa had the highest level of flexibility but less strength. This research contributes to a deeper understanding of how geometric design and resin characteristics impact the mechanical performance of 3D-printed prototypes. By showing these relationships, this study provides valuable insights for optimizing material selection and geometric design to meet specific application needs, ultimately advancing the field of additive manufacturing.

MECHANICAL EVALUATION OF VARIOUS GEOMETRICAL DESIGNS IN ADDITIVE MANUFACTURING FOR FUTURE KNEE BRACE HARNESS.

by

Paul Modey

A Thesis
Submitted to
The Faculty of The Graduate School at
The University of North Carolina at Greensboro,
in Partial Fulfillment
of the requirement for the Degree
Master of Science

Greensboro

2024

Approved by

_____

Dr. Dennis LaJeunesse
Committee Chair

APPROVAL PAGE

This thesis written by Paul Modey has been approved by the following committee of the Faculty of The Graduate School at The University of North Carolina at Greensboro.

Committee Chair _____

Dr. Dennis LaJeunesse

Committee Members _____

Dr. Eric A. Josephs

_____

Dr. Daniel Herr

4/23/2024

Date of Acceptance by Committee

4/23/2024

Date of Final Oral Examination

ACKNOWLEDGEMENTS

My first and foremost gratitude goes to the Almighty God the Father, the Son and the Holy Spirit for guiding me throughout my journey in the Nanoscience program at the University of North Carolina at Greensboro. I also want to thank the able faculty members of the Joint School of Nanoscience and Nanoengineering for their immense support throughout my studies.

Secondly, I want to thank Dr. Denis LaJeunesse, my supervisor, for giving me the opportunity to train under him and work in his project. I am also grateful for his support with through his graduate research assistantship which helped to make my graduate studies possible. His constant support, words of encouragement and direction has kept me energized throughout this work. I extend my gratitude to Mr. Adnan Karim, Mr. Shadrack Boadu Afrane and Mr. Hunter Holden, PhD for also guiding me on this journey by sharing their ideas and expertise to make my work easier.

Finally, I want to thank Dr. Daniel Herr and Dr. Eric A. Josephs for accepting to be on my committee and offering to give their sincere feedback on my work. Their contribution helped to give this work a better outcome.

TABLE OF CONTENTS

LIST OF TABLES

LIST OF FIGURES

CHAPTER I: INTRODUCTION

1.1 Background

Additive manufacturing also known as 3D printing or rapid prototyping since its invention has been improved over the years (Gross et al, 2014). It has a wide application ranging from industrial, aerospace to medicine. This form of manufacturing gained more attention over the years due to its unique ability to produce objects or prototypes that are easily customizable with complex geometries as compared to conventional ways of manufacturing (Pattinson et al, 2019). Traditional fabrication methods for orthopedic devices, including custom-made splints, have seen limited improvement over the years, leading to redundant and less preferable solutions for injury prevention and joint support. Industrial processes or manufacturing techniques have in response improved to ensure an improvement in quality, efficiency, and functionality of products with reduced costs of production. A leading method in this evolution is Additive manufacturing generally known as three-dimensional printing (3D printing).

Additive printing, also known as rapid prototyping, involves the layer-by-layer manufacturing technology whereby materials (inks) are deposited progressively to form digitally designed models. Since its insurgence in 1986, this industry has seen an improvement and has helped made the production of devices more functional, less complex, and more customizable. Through the help of computer aided design (CAD)or computer-aided manufacturing software (CAM), it is now easy to print out models that have been predesigned. Through the help of CAD software such as AutoDesk, AutoCAD, SolidWorks, Creo Parametrics and OpensCAD, an original design of prototypes are drafted and later Converted to .STL (Standard Tessellation Language or Stereolithography) format. The .STL format which has been established by Charles Hull as the gold standard gives the designed prototype readability by the 3D printer (Gross et al, 2014).

1.2 Types 3D Printing

Different types or methods of additive printing have been developed and improved over the years. These types of 3D printing can broadly be categorized into three (3) groups such as Laser printing, Extrusion printing and Inkjet printing (Li et al, 2020). The sub-categories under these 3 major types include but not limited to Stereolithography which utilizes photopolymers in the presence of light (UV), fused deposition modeling (FDM) and Inkjet printing which uses various powders to print materials (Renjier et al, 2010). The method or type of printing selected depends on factors such as goal of the intended object to be developed, available materials, ease of use amongst others given that these methods have their own limitations or disadvantages (Renjier et al, 2010, Leukers et al, 2005). The following paragraphs talk about the various types of 3D printing in detail.

1.2.1 Laser Printing

Laser printing is the most common group amongst the types of 3D printing. This method works through a buildup of light energy in a consecutive manner. The sub-groups under this method include stereolithography, two-photon polymerization and laser induced forward transfer (Li et al, 2020).

1.2.2 Stereolithography

This is the pioneer of the field of laser type of printing. This was first developed by Charles Hull (C.W. Hull, Google Patents (1986) US 4575330 A) at 3D systems in the 1980s and has a set-up that has four components: a container that has a photocurable resin, a light source which is usually UV light that induces polymerization and crosslinking, a system that controls the horizontal plane movement of the light and another system that controls the vertical plane movement of the print platform. The light source cures a photopolymer resin in a layer-by-layer

manner by absorbing photons at a depth that is mostly greater than the height of the platform on which the fabrication is done (Li et al 2020). The platform moves in the Z-direction after the deposition of each layer of resin to produce a 3D construct with 30μm resolution (Mondschein et al, 2017). A major advantage of this method is the ability to produce fine prints in a rapid manner.

1.2.3 Two-Photon Polymerization

Two-photon polymerization employs ultra-short laser pulses in the near-infrared spectrum, specifically using a titanium: sapphire laser operating at a wavelength of 800 nm, to start the polymerization process of a light-sensitive substance within a focused area (Xing et al 2015

1.2.4 Laser-Induced Forward Transfer

The laser induced forward transfer consists of 3 main components which are a pulsating laser directed at a slender metal layer or similar materials with high laser absorption capability (such as hydrogels), a source substrate (transparent quartz or glass ribbon) that supplies the laser-absorbing materials, and a recipient substrate for the inks (Li et al 2020). This method of printing is very ideal for cell printing and has been applied and improved over the years.

1.3 Materials In 3D Printing

Synthetic polymers are preferred to natural polymers when it comes to their application in biomedical engineering steers on the advantages they possess over the natural polymers. For instance, Biswas et al found natural polymers to possess poor mechanical properties as compared to synthetic biopolymers. Another disadvantage outlined in their work is the difficulty in large scale production of natural polymers (Biswas et al, 2022). Synthetic polymers such as photopolymer resins are used in 3D printing. These are polymers which are chemically derived from naturally occurring polymers or other forms of synthetic monomers (Shiva et al 2023) are designed specifically to possess properties and functions of biopolymers which are found in cells.

This gives these polymers the abilities to be applied in the field of medicine and biomedical engineering. An example is seen the recent exploration of hydrogels in the field tissue engineering, regenerative medicine, and flexible wearable electronics (Li et al, 2020). This is possible because of the ability of these hydrogel polymers to exhibit properties such as biodegradability, good mechanical properties like natural tissues and their ability to not produce long term immune-related inflammation. Other characteristics that make synthetic polymers to be employed in making resins is the ability of their functional groups to form crosslinks when exposed to a light source such as the UV light.

1.4 Significance and Application of AM in Medicine and Health

The significance of AM has been seen in fields spanning aerospace, architectural, engineering, medical and consumer goods industry. Applications of AM in the medical field can be seen in facial reconstruction, bioprinting of tissues for surgical reasons, orthodontics, prosthetics, and orthotics amongst others. For instance, AM or 3D printing has become an attractive method of developing scaffold for tissue replacement and tissue regeneration (Gross et al, 2014). This is due to the advantage it has shown over traditional methods of by enabling the development of biocompatible materials that are resorbable (Rengier et al, 2010). Another application of AM is seen in the production of prosthetic and orthotic wearable devices which has also seen an improvement in recent years. An example was demonstrated by Pattinson et al in 2019 where they manufactured biomechanically tailored meshes for compliant wearable devices using 3D printing. Their results showed that orthotic devices can be customized to possess tissue-like properties, and this confirmed one of the main advantages AM has over the traditional manufacturing of wearable orthotic devices. Another example of the application of AM in the field of wearables was demonstrated in the development of running shoes which are ultralight weight

thereby improving performance of runners (Silbert, 2019). Customization of wearable devices using traditional or conventional methods is time consuming, tedious and offer less compliance to users when compared with AM (Blaya et al, 2018). This attribute was emphasized by Simon Fried in his article, 3D printing Medical Devices: Considerations for wearables and implants, where he stated the need for prosthetics to be developed specifically for patients. This has led to the manufacturing world shift more and more towards the use of AM to produce wearable orthotics and prostheses.

1.5 Mechanical Properties and Tensile Strength Testing

A critical characteristic of performance in wearable of support devices is their mechanical characteristics. Poorly fitting, rigid, and bulky support devices can lead to discomfort and poor performance and most of these attributes can be found in conventionally manufactured support devices such as ankle and knee braces. An instance was demonstrated by Kingsnorth and LeBlanc in 2003, where they found implanted surgical meshes used for mechanical support for healing tissues after hernia surgeries to have caused abdominal rigidity and discomfort. It has therefore become very imperative to consider the biomechanical properties of additively manufactured products. This importance was demonstrated by Soe et al in 2015 when they worked on the feasibility of optimizing bicycle helmet design safety. According to them, since bicycle helmets are developed to reduce impact of forces on the head, they need to be to possess the necessary energy dissipating components. Their work therefore focused on the manufacturing of thermoplastic elastomer (TPE) as the energy-dissipating component of the bicycle helmet using laser sintering process. Through appropriate testing of tensile and compressive strength, the were able to optimize the compressive strength of the inner liner of the helmet that was produced additively (Soe et al, 2015).

The established standard for testing plastic materials was developed by the American Society of Testing and Materials (ASTM) and has been adopted as a standardized method of determining the tensile and mechanical properties of additively manufactured products. This test is known as the ASTM D638 - 14 Standard Test Method for Tensile Properties of Plastics. This examination holds importance as it furnishes data on the tensile properties of plastic materials, which are primarily valuable for qualitative assessment, research, and development purposes. According to an article published by astm.org, tensile properties of resin-matrix composites which are reinforced with continuous or discontinuous high modulus >20-GPa (i.e >3.0 x 10^6psi) fibers should be done using D3039/D3039M Test Method.

When producing customizable and efficient wearable support devices, it is very crucial to consider mechanics of soft tissues. This can be very challenging considering the non-linear behavior of soft tissues such as muscles and tendons. It is very important to consider characteristics such as tensile stress and strain which vary as these tissues stretch or recoil (Calvo et al, 2010). Variation in these characteristics is not only seen at the tissue level but also varies from individual to individual based on body type. Besides mechanical properties, other properties that should be considered when developing wearable support devices such as knee sleeves is breathability as this helps to avoid issues such as irritability from sweating or trapping of sweat under the brace.

1.6 Problem Statement

Conventional methods of fabrication of support braces uses fabric which are knitted and weaved. These conventional methods have over the years seen significant innovations to improve the quality of fabrics produced and a prominent work in this field was done by McCann et al in 2016 where they produced a compiler that was able to allow knit objects to be scheduled, scaled, and otherwise shaped in ways that require thousands of edits to low-level instructions. Their

algorithm facilitates the conversion of broad shaping and scheduling tasks into detailed, precise actions at a granular level to produce better and more advanced fabrics. Although these advancements have shown some level of improvement, knitting and weaving poses a limitation in fabrics when it comes to sharp gradients in mechanical abilities as compared to 3D printing. Another limitation found from research was the reduced stiffness and control offered by the looped topologies used in knitting (Pattinson et al, 2019).

AM has been applied in the manufacturing of meshes for wearable braces in the ankle joint. An example of this application was demonstrated in the work of Pattinson and his colleagues where they employed additive manufacturing to produce biomechanically tailored meshes for wearable ankle and hand braces. They demonstrated how explicit programming of the toolpath in an extrusion AM process can enable new, flexible mesh materials having digitally tailored mechanical properties and geometry. Their work however focused on one geometry and did not seek to address what effect different geometries might have on the mechanical properties. Their work also did not employ different printing materials or polymers and hence could not tell if the specific polymer used influences the geometry. To address these limitations, this research aims to investigate the biomechanical properties of additively manufactured meshes for knee sleeves. Also, this work focused on comparing different geometries to know which geometry presents the best mechanical property for mass production. Below are the specific objectives and the gaps this work seeks to fill.

1.7 Objectives

Specifically, this study seeks to:

1. Analyze the effects of different geometries on the biomechanical properties of additively manufactured inserts (meshes) for a next generation medical device (knee sleeve).

2. Analyze the effects of different synthetic polymer resins on the biomechanical properties of the additively manufactured meshes.
3. Provide necessary background to developing a next generation knee sleeve that can be customizable and more efficient in preventing knee injuries.

CHAPTER II: METHODOLOGY AND MATERIALS

2.1 Study Site.

The study was conducted in the Genomic lab at the Joint School of Nanoscience and Nanoengineering. This is a multidisciplinary lab that is equipped with state-of-the- arts equipment rendering it conducive for conducting successful projects. Prior to commencing the research, training sessions were conducted to ensure safety protocols and equipment operation, facilitating the smooth execution of the study.

2.1 Study Design.

A cross sectional study design was used to analyze the mechanical properties of different geometrical designs.

2.2 Equipment and Materials.

These materials and equipment were used for the study, Elegoo mars 3 3D printer, elegoo mars 3 compatible resins, Elegoo wash and cure station, texture analyzer, and a computer aided design (Openscad, chitubox).

2.2.1 Elegoo Mars-3 3D Printer

Elegoo is a company known for providing affordable and high-quality resin 3D printers. The Elegoo Mars 3 3D series, launched in 2022, was utilized for this research. This is a user-friendly printer released as the first ultra-precision 3D printer with an LCD display that allows seamless operation. The equipment is equipped with a 6.6-inch ultra 4K monochrome LCD display and a 2.0 printing film which provide high precision, visuals, adhesion, and stability of printed layers. The printing technology employed in this equipment is Stereolithography, and it uses UV light with a wavelength of 405nm to enable the photopolymerization process, where liquid resin is solidified layer by layer to create complex 3D objects. It has a print time ranging between 1.5 to

3 seconds which offers efficient and rapid production capabilities. The ELEGOO Mars 3 is equipped with the capability to print materials with a remarkably small layer thickness of just 0.01mm. This feature played a pivotal role in its selection for this research project. A notable difference between this machine and conventional 2K LCD 3D printers is its larger printing volume, which surpasses that of the Mars 2 by 37%. Additionally, it boasts an XY precision of up to 35 microns, representing a 30% increase compared to the Mars 2. Furthermore, it demonstrates higher printing efficiency while demanding less maintenance. The equipment includes an air purifier with a built-in active carbon filter, designed to efficiently absorb and filter resin odors and strong fumes, ensuring a fresh and pleasant printing environment.

Fig 2. 1 Elegoo Mars-3 3D Printer

2.2.2 Wash and Cure Station.

This station serves as a post-processing station for the removal of surplus resin from printed objects, followed by curing to enhance the mechanical properties of the materials. It comprises two machines known as the Elegoo Mercury XS bundle. The initial component is designed for the washing phase and is equipped with a reservoir containing Isopropanol or alcohol. This solution effectively cleanses the printed objects by eliminating any excess uncured resins, thereby ensuring thorough cleaning prior to the curing process.

The other component of the station features an UV-LED light source, essential for initiating the curing process. This light emits a wavelength that activates the resins within the printed objects, facilitating the curing process. It also includes a rotating platform mechanism, ensuring uniform exposure of the objects to the UV light from all angles. This process facilitates the drying and solidification of the resin within a specific timeframe.

The image below shows a picture of the wash and cure station.

Fig 2. 2 The Wash and Cure Station Process

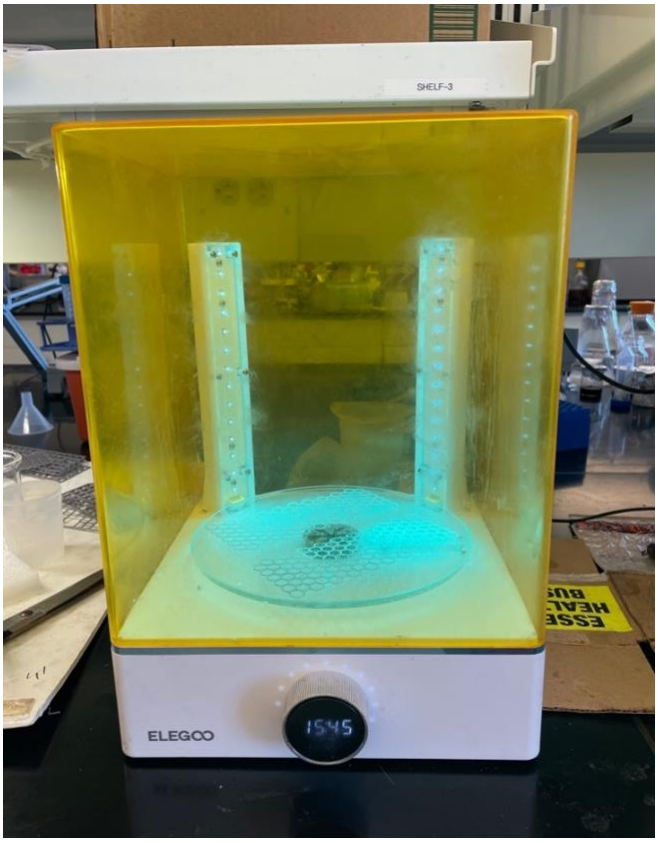

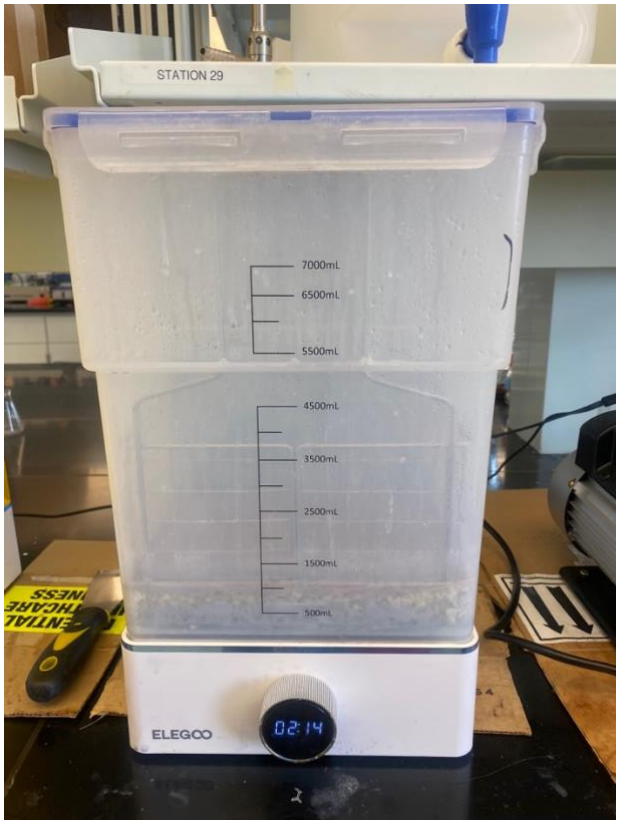

2.2.3 Photopolymer Resins

Resins exhibit UV reactivity and undergo rapid polymerization upon activation. They are commonly classified into several categories, including standard, engineering, dental, medical, castable, and biomaterial resins. This project specifically centered on the utilization of five unique types of Elegoo Mars 3 compatible resins. These resins comprise thermochromic, water washable(grey), standard translucent photopolymer, standard plant-based photopolymer (grey), and ABS-like resins (light blue). Five different types of resins were selected for diversity and comparison since each resin has different parameters for printing. These parameters are listed below.

1. Thermochromic Resin

At a temperature of 50 degrees Celsius, this resin changes color from grey to purple.

Parameter settings for slicing into Chitubox:

Exposure time= 7s

Bottom exposure time = 45s

Lift distance (mm) = 5

Layer height (mm) = 0.05

Lift speed (mm/min) = 110

Retract speed (mm/min) = 280

2. Water washable(grey)

Parameter settings for slicing into Chitubox:

All sample designs were printed perfectly with no difficulties.

Exposure time= 6s

Bottom exposure time = 60s

Lift distance (mm) = 5

Layer height (mm) = 0.05

Lift speed (mm/min) = 110

Retract speed (mm/min) = 280

3. Standard translucent photopolymer.

Parameter settings for slicing into Chitubox:

Exposure time= 3s

Bottom exposure time = 45s

Lift distance (mm) = 5

Layer height (mm) = 0.05

Lift speed (mm/min) = 110

Retract speed (mm/min) = 280

4. Standard plant-based photopolymer (grey)

Parameter settings for slicing into Chitubox:

Exposure time= 5s

Bottom exposure time = 70s

Lift distance (mm) = 5

Layer height (mm) = 0.05

Lift speed (mm/min) = 110

Retract speed (mm/min) = 280

5. ABS-like resins (light blue)

Parameter settings for slicing into Chitubox

Exposure time= 2.5s

Bottom exposure time = 35s

Lift distance (mm) = 5

Layer height (mm) = 0.05

Lift speed (mm/min) = 80Retract speed (mm/min) = 21

2.2.4 Computer Aided Design.

This study utilized an OpensCad version 2021.01 to design all prototypes in a 3D format. OpensCAD is a free software that is used for creating solid 3D objects. It has series of programming commands for geometry and operation that allows for control over the design process. Chitubox version 1.9.0 which is a slicing software was also used to prepare the 3D files for printing by slicing them into thin layers for the printer to understand and print.

2.2.5 Texture Analyzer.

The Stable Micro System analyzer was utilized to evaluate the tensile strength of all printed materials in this study. With precise force and displacement sensors, this instrument enabled accurate testing of tensile strength. It is also capable of conducting compression force tests and analyzing textile profiles. Renowned for its user-friendly interface, it does well in assessing the mechanical properties of diverse materials.

Fig 2. 3 The Stable Micro System Analyzer

2.3 Designing of Prototypes.

The sample prototypes were initially sketched in Microsoft Word, after which the 3D images were developed using OpensCAD software. The subsequent section outlines the geometries and dimensions utilized in this research and how they appeared after the designing process in OpensCAD.

The dimensions used were X-150mm, Y-50mm, Z-1mm.

Fig 2. 4 Images Showing Openscad Designs of Selected Prototypes: A. Simple Grid With Holes, B. Hexagonal Grid And C. Zig-Zag

A.

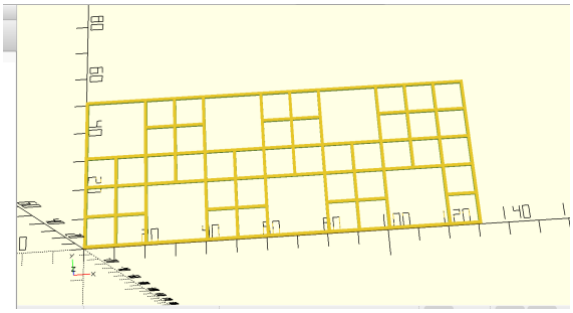

B.

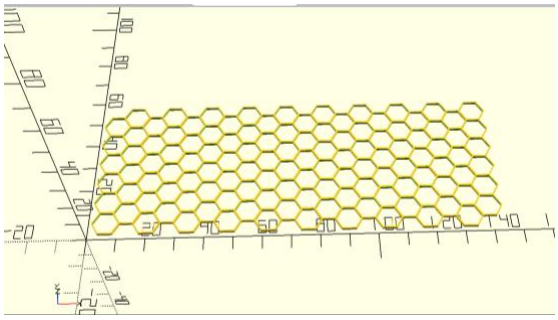

C.

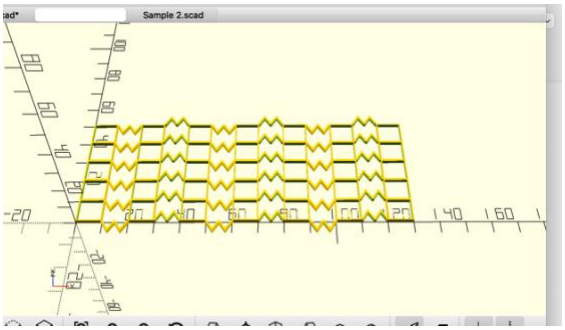

2.4 Printing and Testing Process

- Printing of materials began after the proposed geometries in 3D utilizing the openSCAD software version 2021.01.
- Files were then converted to STL format and sliced using chitubox version 1.9.0 to ensure compatibility with the printer.
- The prototypes were transferred onto a pendrive and subsequently loaded into the Elegoo Mars 3 3D printer to initiate the printing process.
- The duration of each print was recorded for every geometry type and resin variant.
- Upon completion of the printing process, the prints underwent a washing procedure in an alcohol container to remove any excess material, followed by removal from the Elegoo Mars 3 3D printer platform using a scraper.
- Subsequently, the prints were exposed to UV light for 20 minutes to enhance drying and optimize mechanical properties.
- The materials underwent testing utilizing a texture analyzer known as the Stable Micro System.
- Prints were inserted into the machine, and parameters were configured to record the tensile strength of each print.
- This sequence of steps was replicated for all 150 printed samples.

2.5 Data Analysis and Representation

Data collected was organized and analyzed in Microsoft Excel version 16.83 and MySQL Workbench version 8.0.33. MySQL was used to write queries to extract data into various tables and analysis and was performed in MS Excel. Results were tabulated and averages were calculated. Figures and graphs were plotted in Microsoft Excel and then copied to Microsoft Word.

CHAPTER III: RESULTS

3.1 Print Times

Different print times were recorded for the different geometries and different photopolymer resins.

Table 1. Table Showing Various Print Times and Averages.

Resin type	Geometry	Print times
Standard Photopolymer Resin (Plant based)	Simple grid with holes	8.1
	Hexagonal grid	8
	Zig-zag	6
Translucent photopolymer resin	Simple grid with holes	5
	Hexagonal grid	5.25
	Zig-zag	5
Water-washable (grey)	Simple grid with holes	8.25
	Hexagonal grid	9
	Zig-zag	9
ABS-like Resin (Blue)	Simple grid with holes	5.25
	Hexagonal grid	5.12
	Zig-zag	6.12
Thermochromic resin	Simple grid with holes	9

	Hexagonal grid	9
	Zig-zag	11
Mean print times		7.27266667
SD		1.96561683

3.2 Printed Meshes

The figures below show the some of the various designs and how they came out. Texture differences were noticed in the various prototypes based on the type of resin used. The Translucent and ABS-like resins produced the prototypes with reduction in thickness as compared to the other three (3) Resins.

Fig. 3. 1 Images of Some Printed Meshes Compared From Different Resin Types: A. Standard Photopolymer Resin (Grey) Print, B. Translucent Resin, C. Water – Washable Resin (Grey), D. ABS-Like And E. Thermochromic Resin

A. 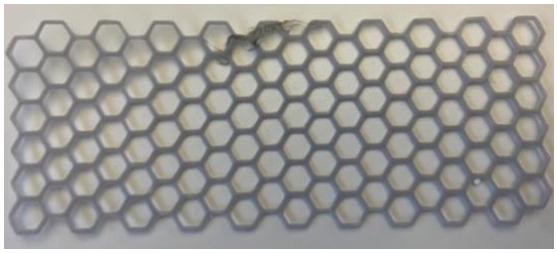

B. 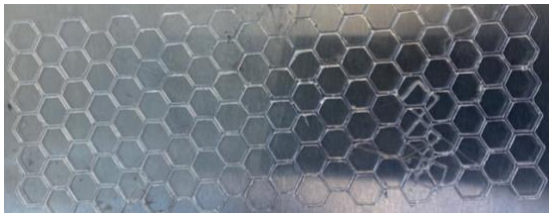

C. 

D. 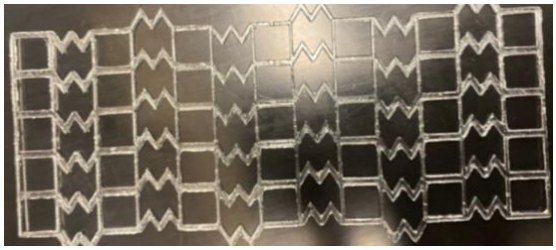

E. 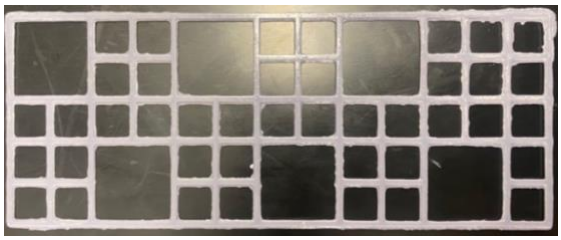

3.2 Mechanical Properties Analysis.

After the mechanical properties were enhanced for each prototype, mechanical properties analysis was performed. Data was collected, organized and stress-strain curves were plotted from the averages of the individual values obtained for 5 prototypes tested. The following results were obtained for the various resin types and prototypes.

3.2.1 Stress-Strain Curve

The tensile stress-strain curve was plotted from the average of individual values from three tested prototypes. The highest peak of Stress in N/mm^2 represents a good tensile property.

(i) Standard Photopolymer Resin.

The grid with holes design had the highest ultimate stress value property with a peak stress value of 2.887 N/mm^2 whilst the geometry with the least peak stress and breaking strain value was the hexagonal grid with a stress value of 1.958 N/mm^2. The Zigzag geometry demonstrated several internal breaks before achieving and final break strain. Below are the plots for the various geometries.

Fig. 3.2. 1 Stress-Strain Plot: Simple Grid with Holes

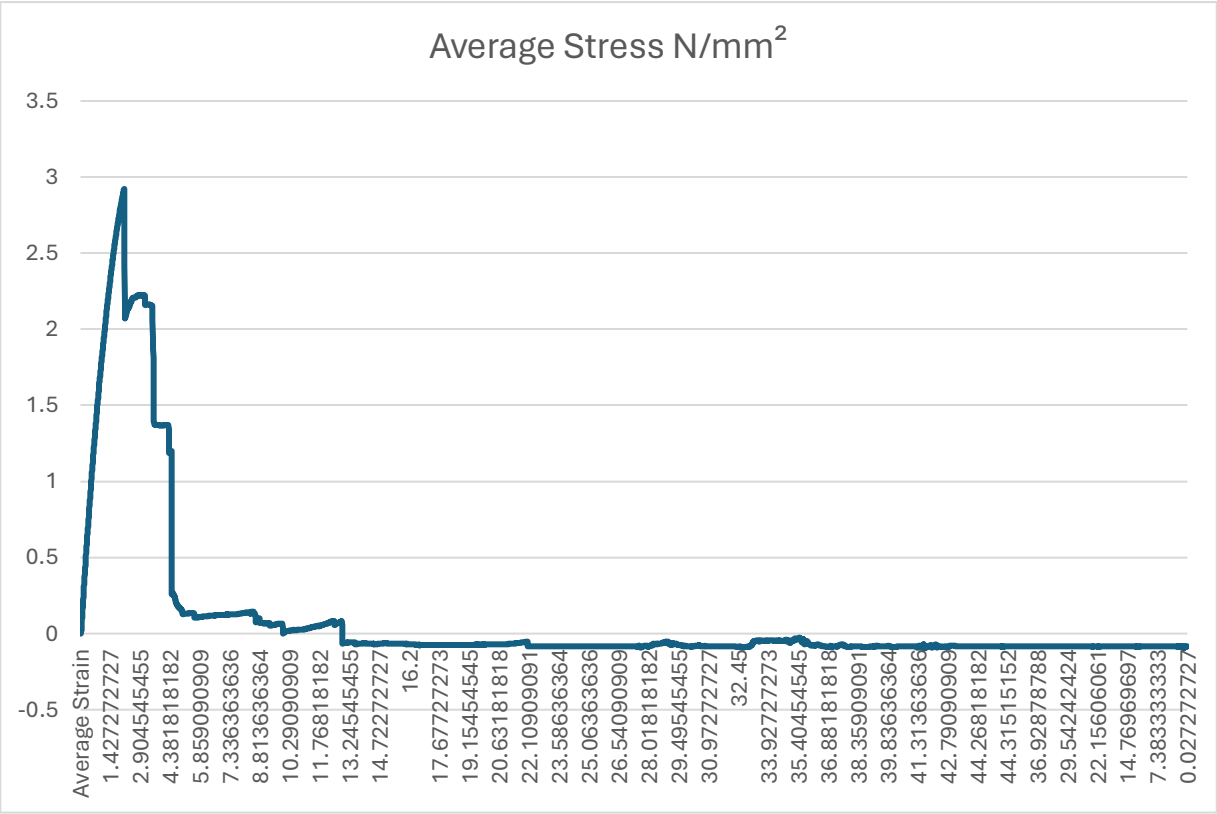

Fig. 3.2. 2 Stress-Strain Plot: Hexagonal Grid

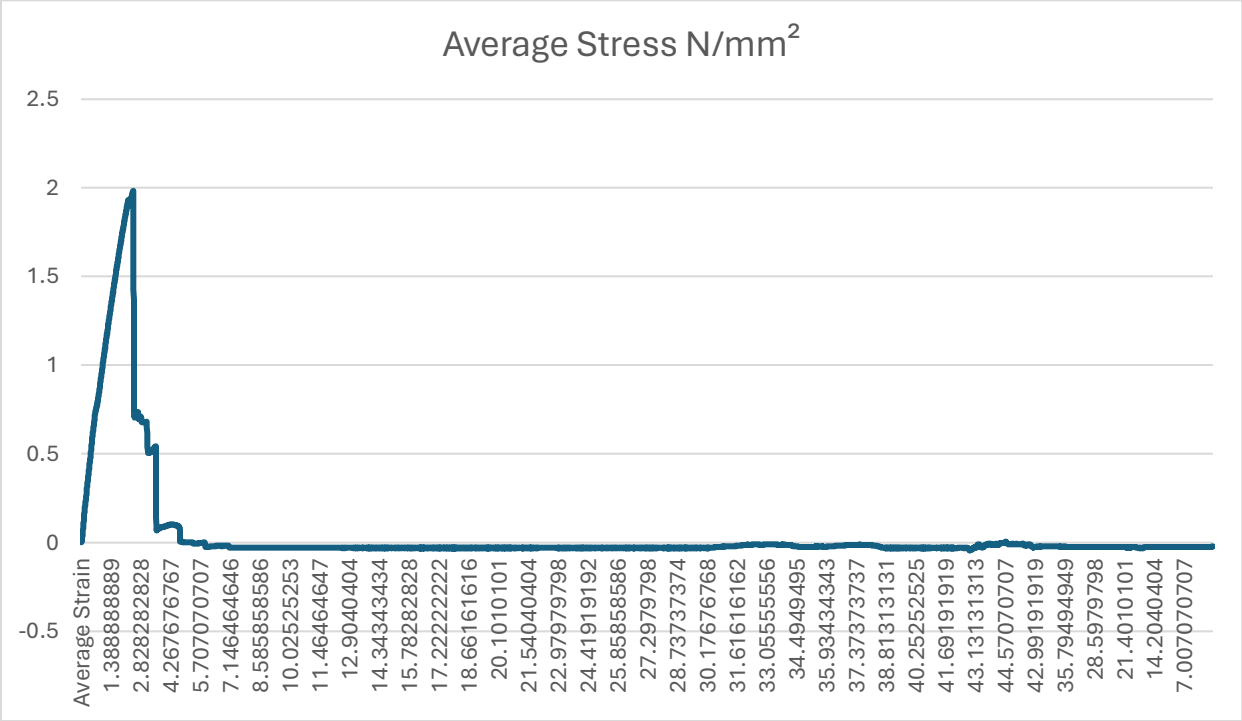

Fig. 3.2. 3 Stress-Strain Plot: Zigzag

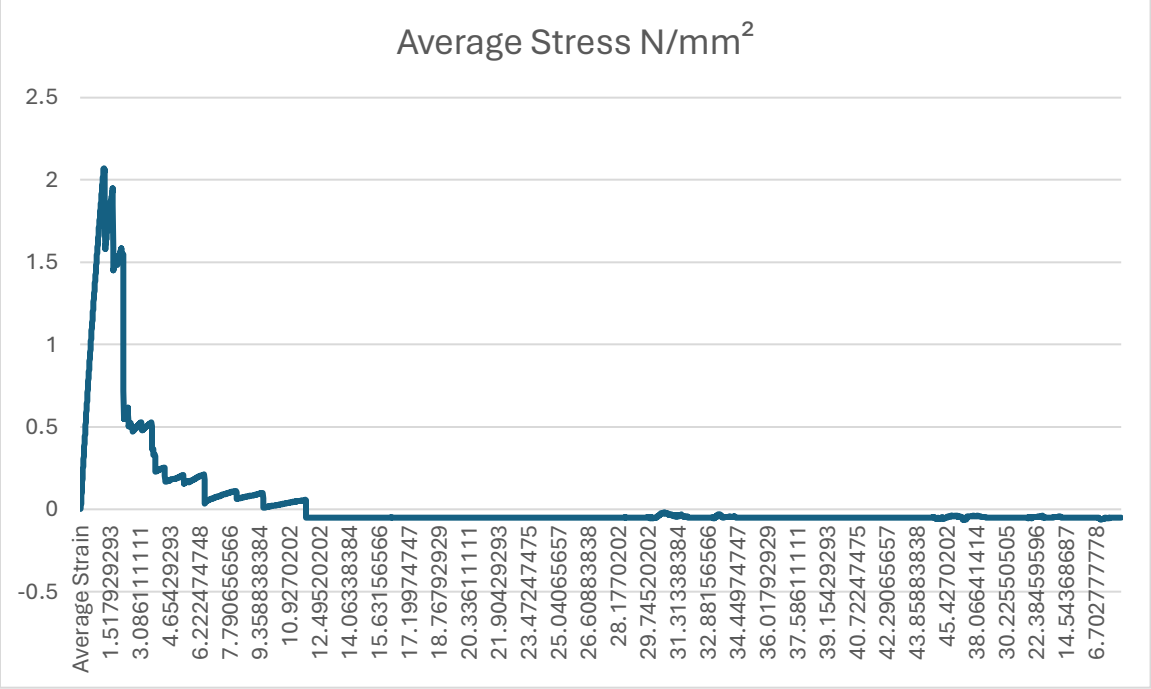

(ii) Translucent Resin

All geometries had multiple internal breakages before a final break. The simple grid design demonstrated the hexagonal grid having a peak stress value of 0.963 N/mm^2. Below are the plots for the various geometries.

Fig. 3.2. 4 Stress-Strain Plot: Zigzag

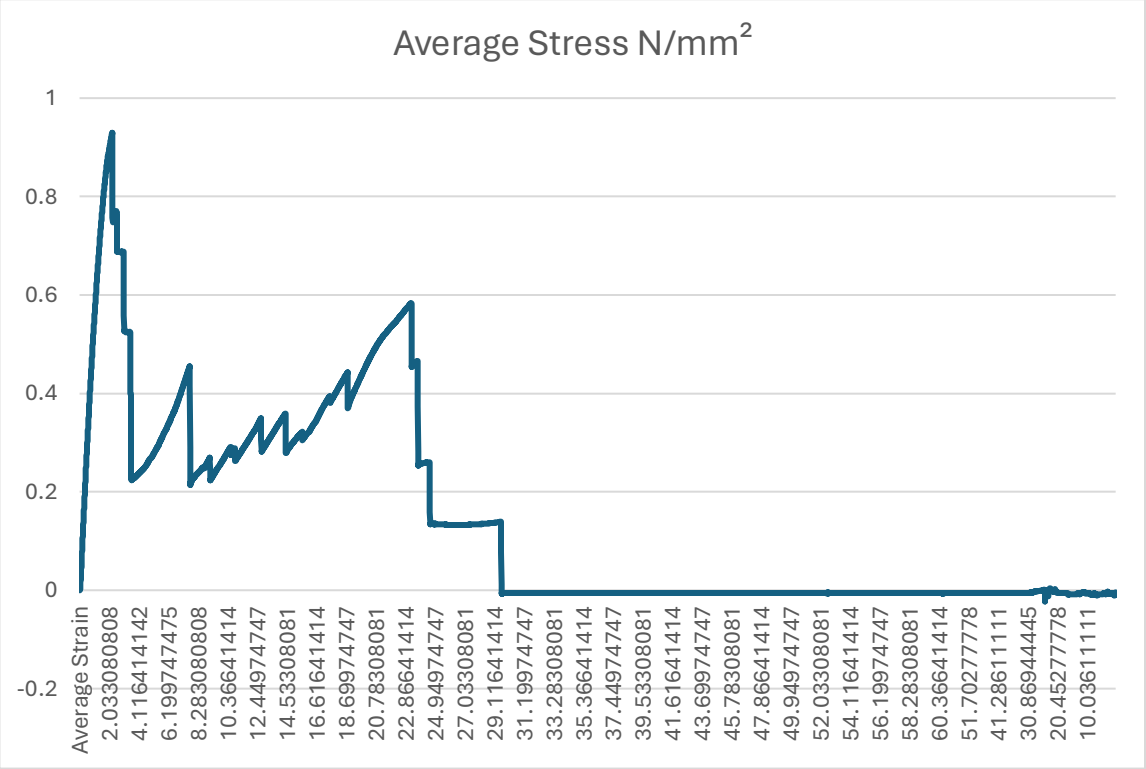

Fig. 3.2. 5 Stress-Strain Plot: Hexagonal Grid

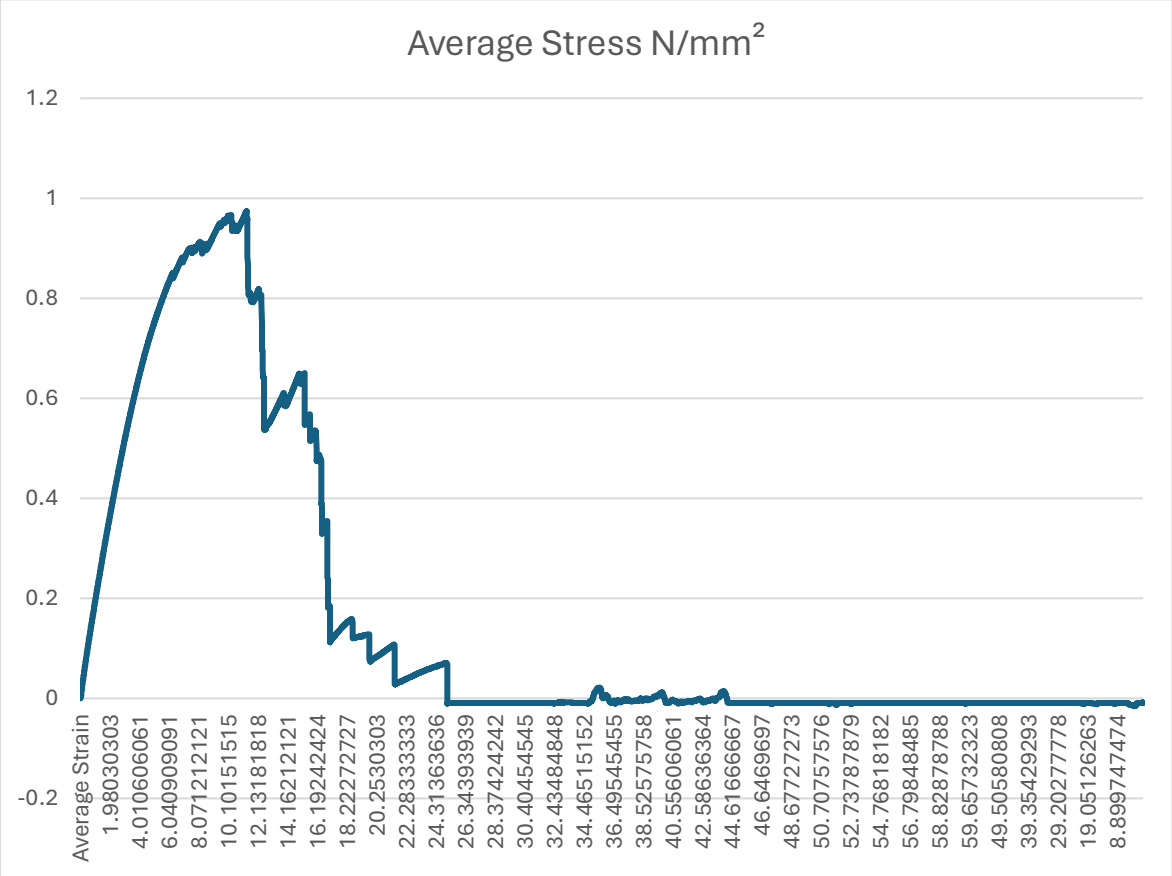

Fig. 3.2. 6 Stress-Strain Plot: Zigzag

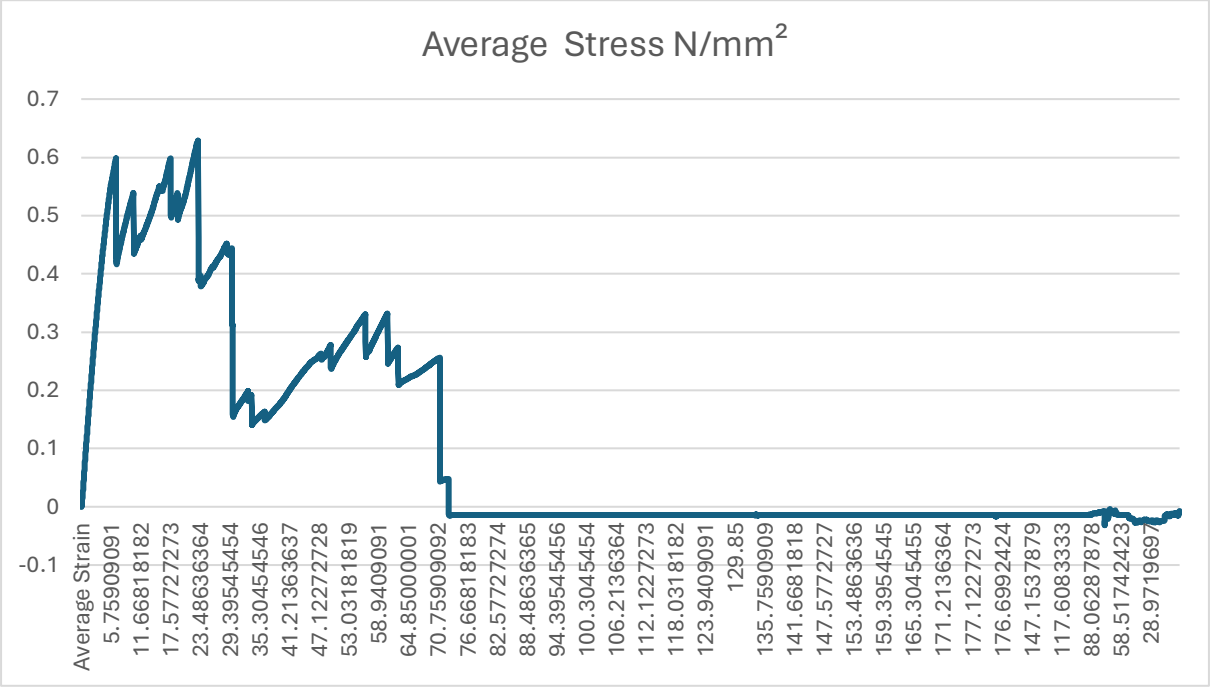

(iii) Water-Washable Resin

The geometries from this resin were most brittle. Simple grid with holes and zigzag geometries had simple breaks with no internal breaks. Simple grid with holes had the highest peak stress value (6.555 N/mm^2) but dropped rapidly to cross the break strain value. Same was seen for the zig-zag geometry whilst the rest of the geometries demonstrated gradual stress-strain curve. The plots are illustrated in the figures below.

Fig. 3.2. 7 Stress-Strain Plot: Grid with Holes

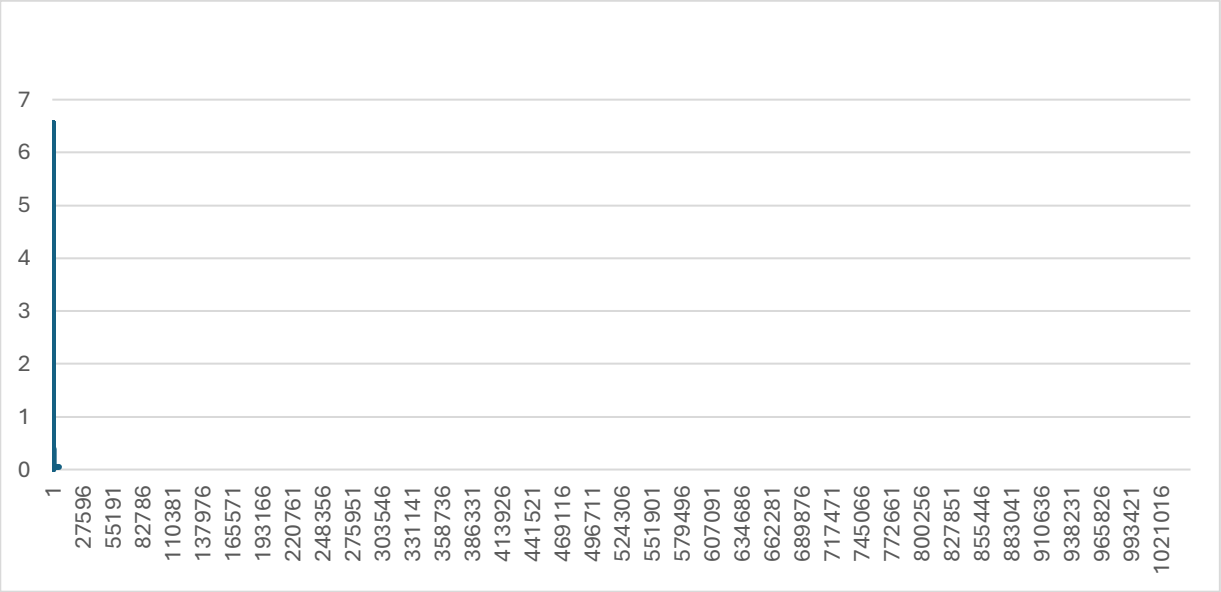

Fig. 3.2. 8 Stress-Strain Plot: Hexagonal Grid

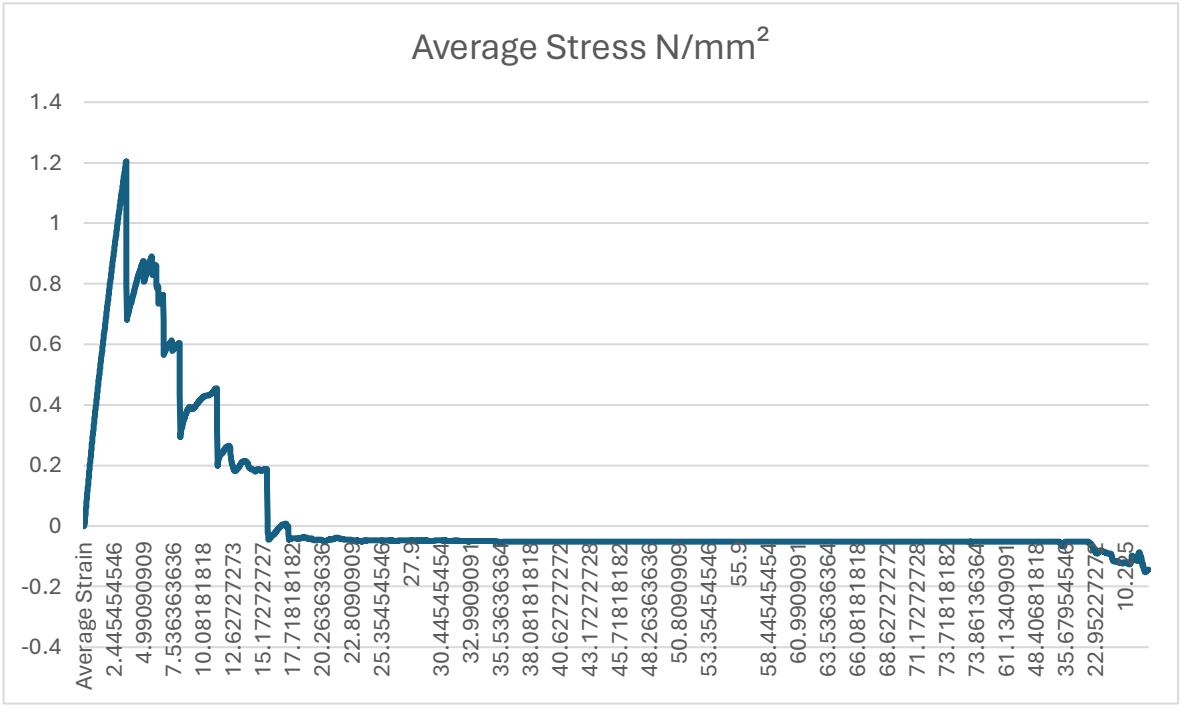

Fig. 3.2. 9 Stress-Strain Plot: Zig-Zag

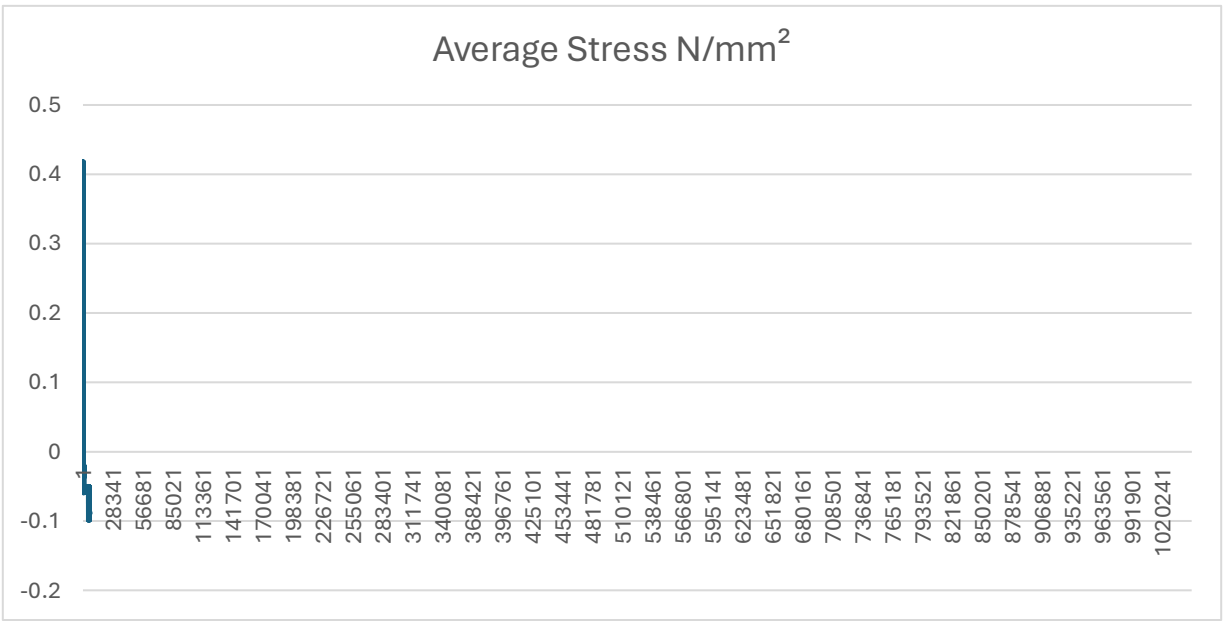

(iv) Abs-Like Resin

For this type of resin, the simple grid with holes geometry had the highest peak stress value (1.980 N/mm^2). The Zig-zag design here had a plot with two peak values with a second peak stress value which is higher than the first linear stress-strain peak value. The rest of the results are illustrated by the graphs below.

Fig. 3.2. 10 Simple Grid with Holes

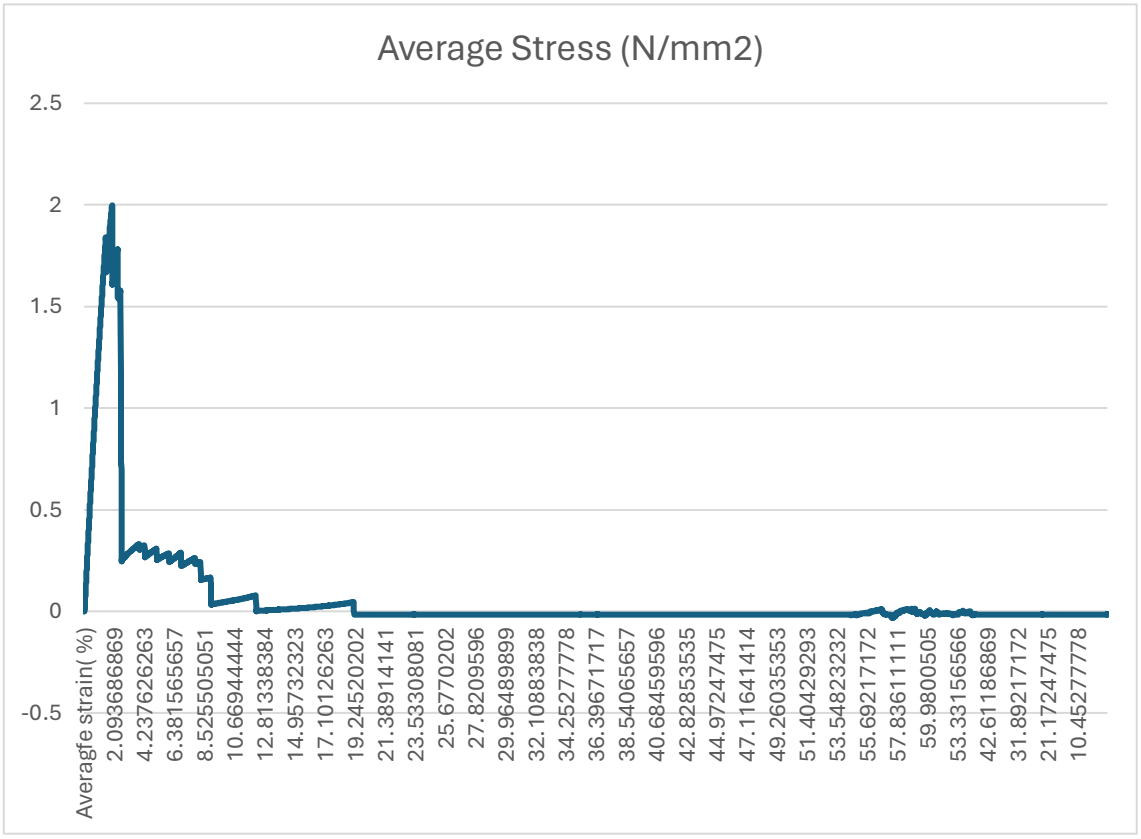

Fig. 3.2. 11 Hexagonal Grid

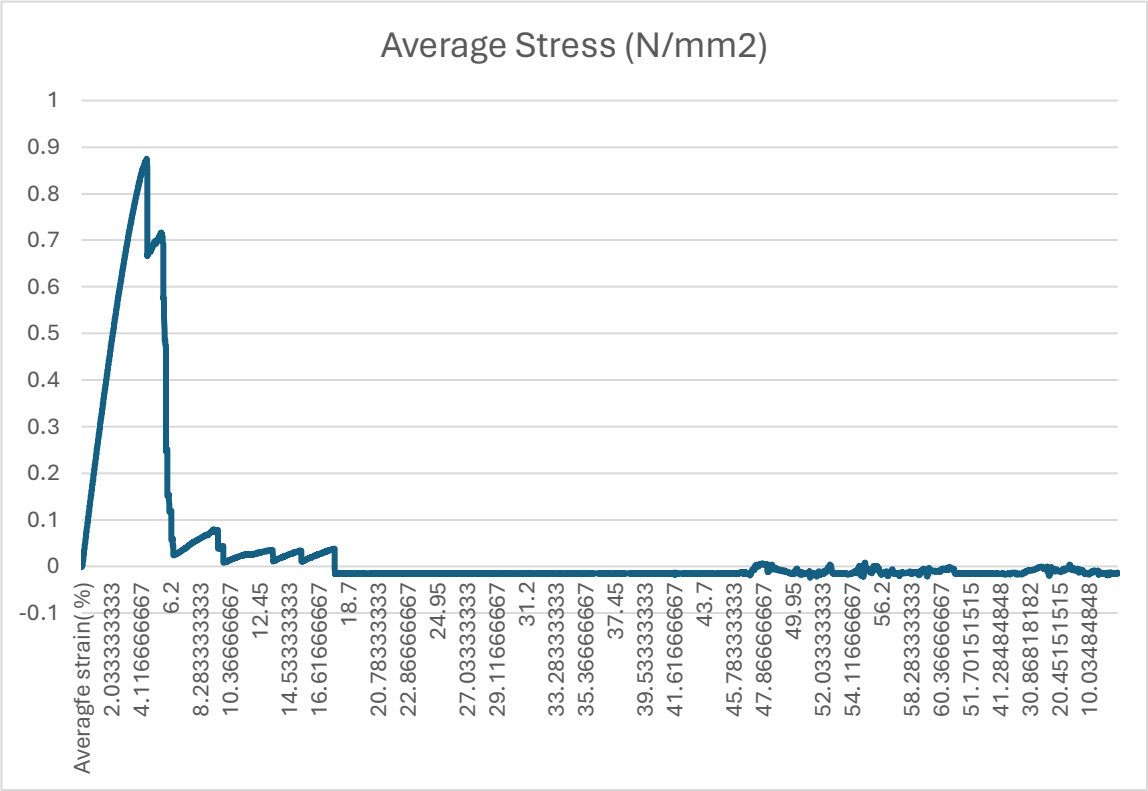

Fig. 3.2. 12 Zig-Zag

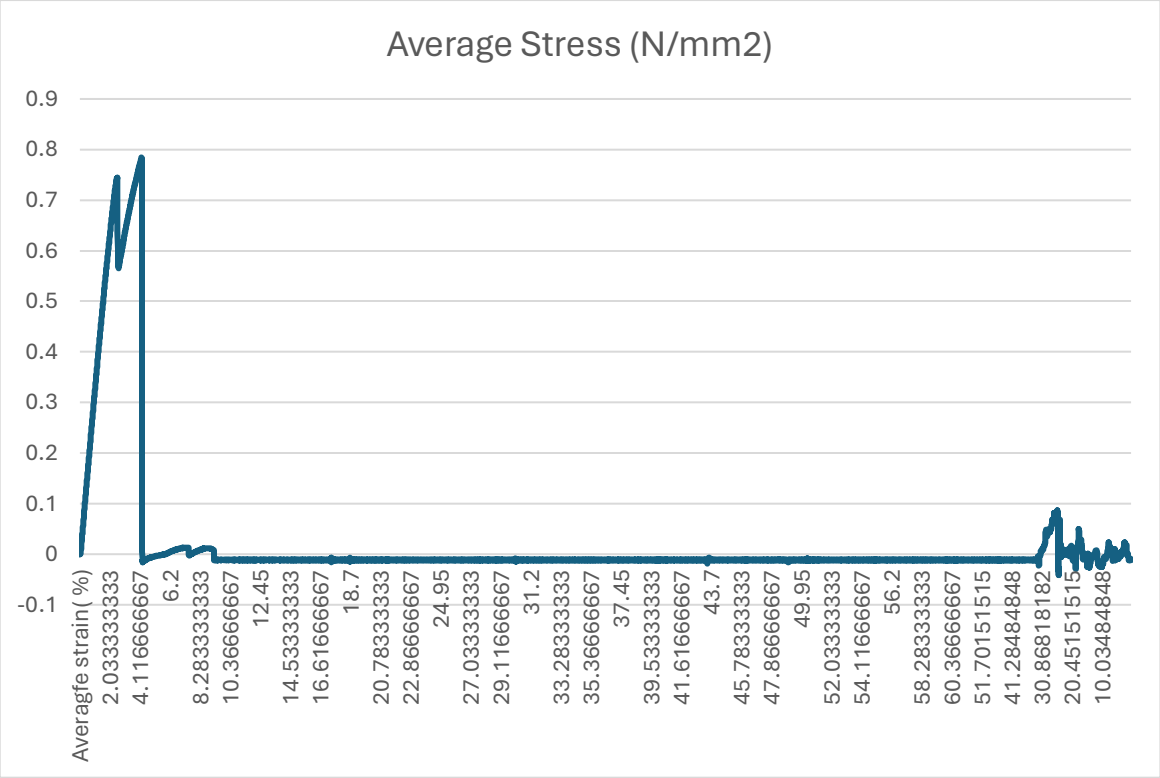

(v) Thermochromic Resin

For this class of resin, the simple grid with holes had the highest peak stress value (3.147 N/mm^2) when compared with the other geometries. The zig-zag geometry showed the greatest ability to undergo a higher amount of strain with several internal breaks before finally attaining a breaking strain value of 12.336%. The rest of the results are presented below:

Fig. 3.2. 13 Simple Grid with Holes

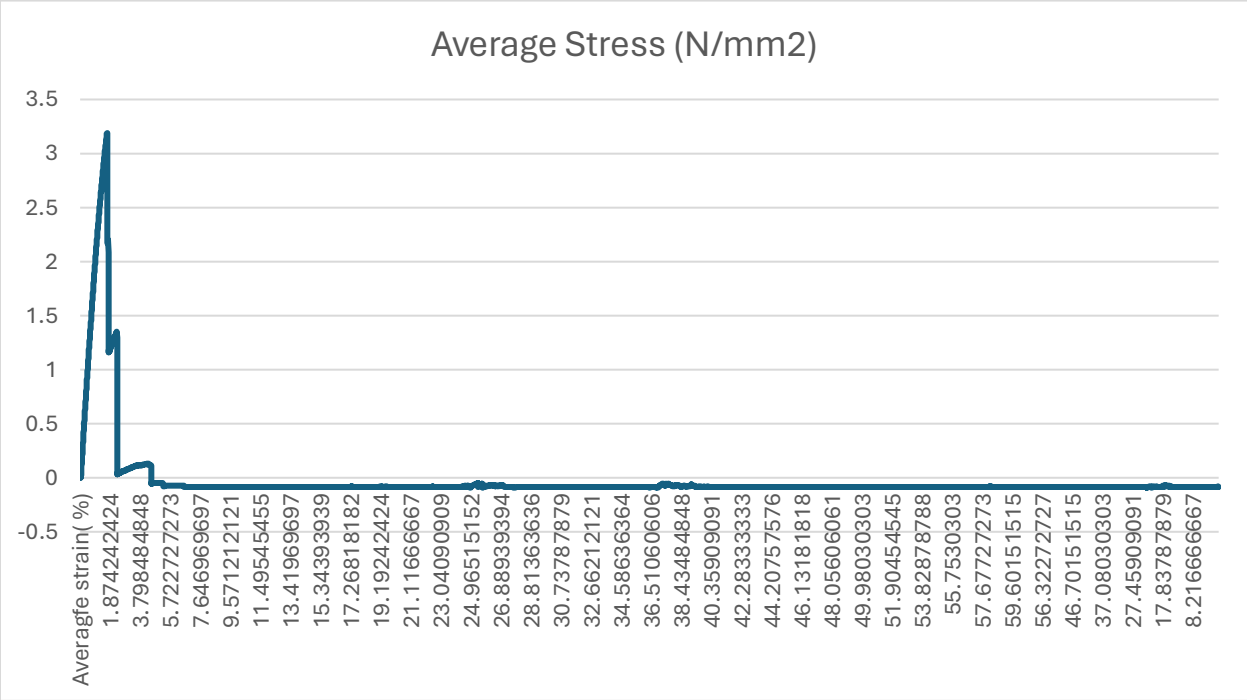

Fig. 3.2. 14 Hexagonal Grid

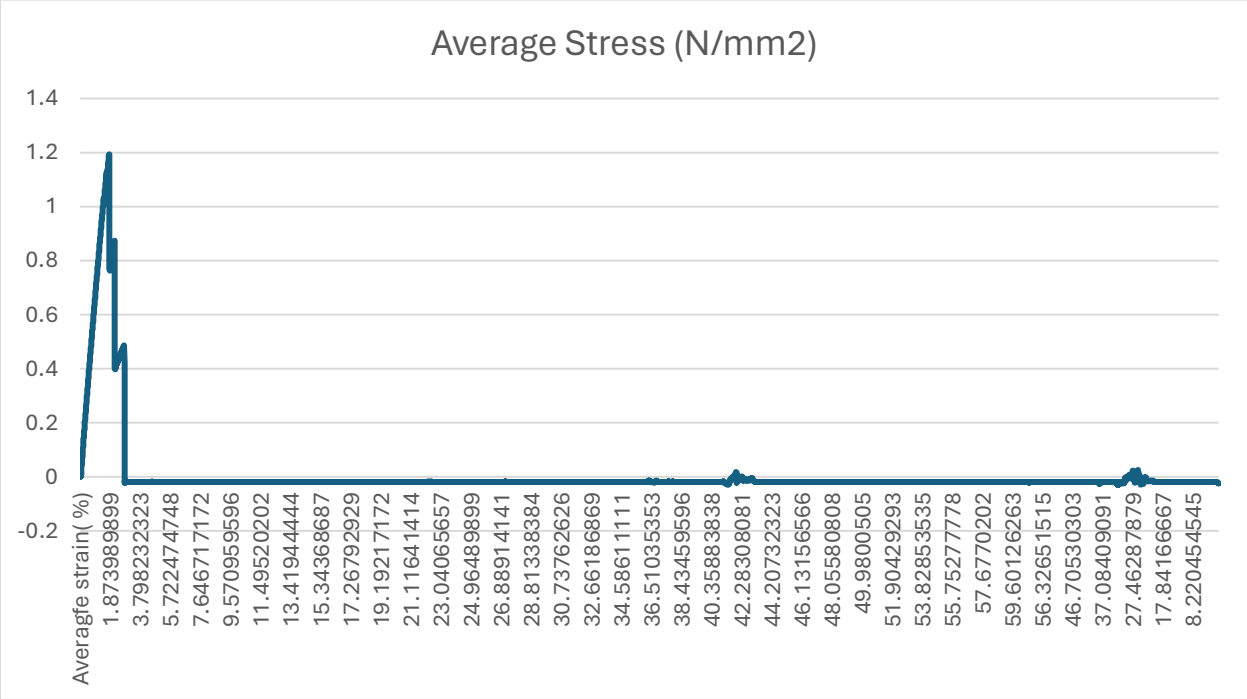

Fig. 3.2. 15 Zig-Zag

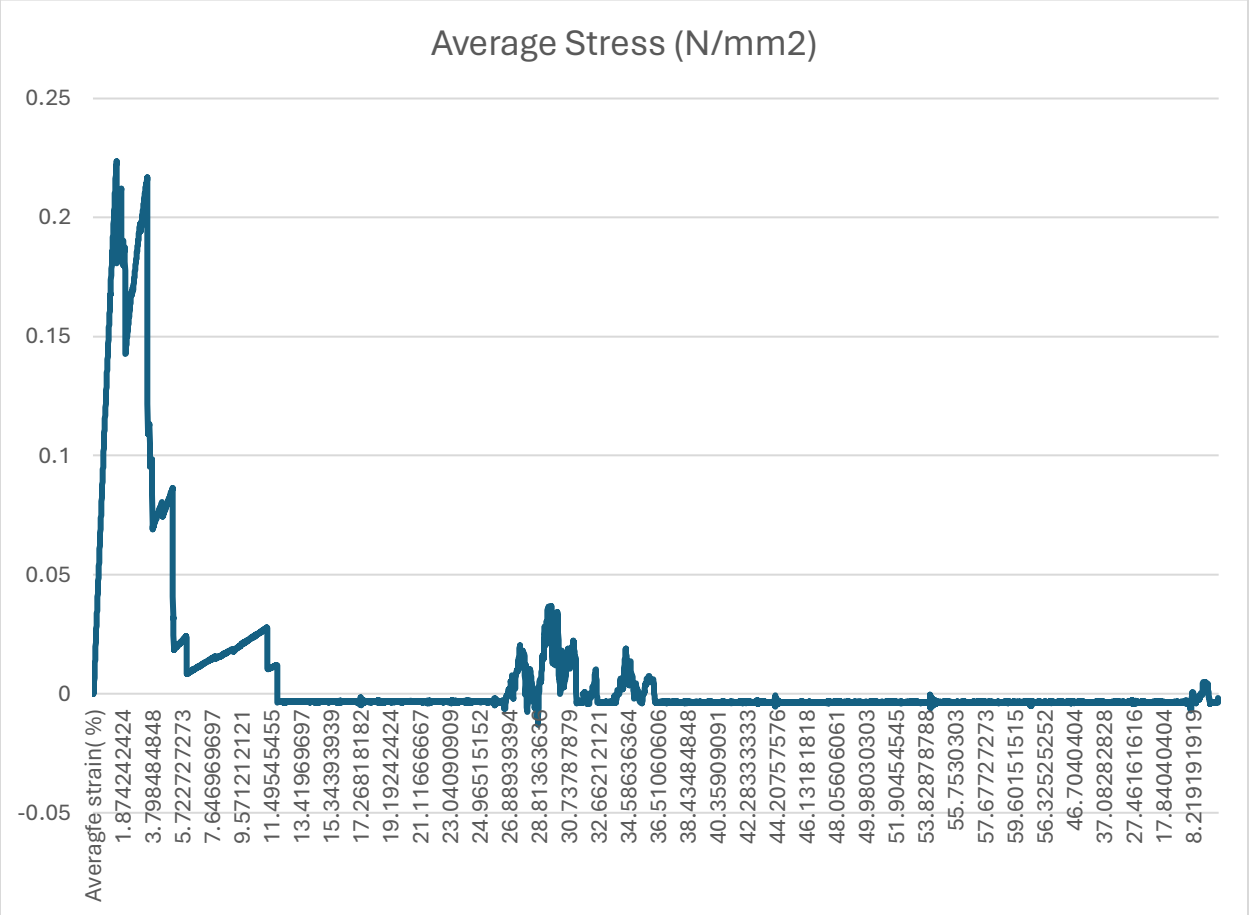

3.3 Young's Modulus Deduction

The Young's modulus of elasticity was deduced for each curve plotted by calculating the slope from the rising linear phase of the curves and the results represented by the bar charts below. Two bar charts were created using the means and standard deviations first, across resins and secondly for the various geometries.

Fig. 3.3. 1 Young's Modulus of Elasticity For The Various Resins

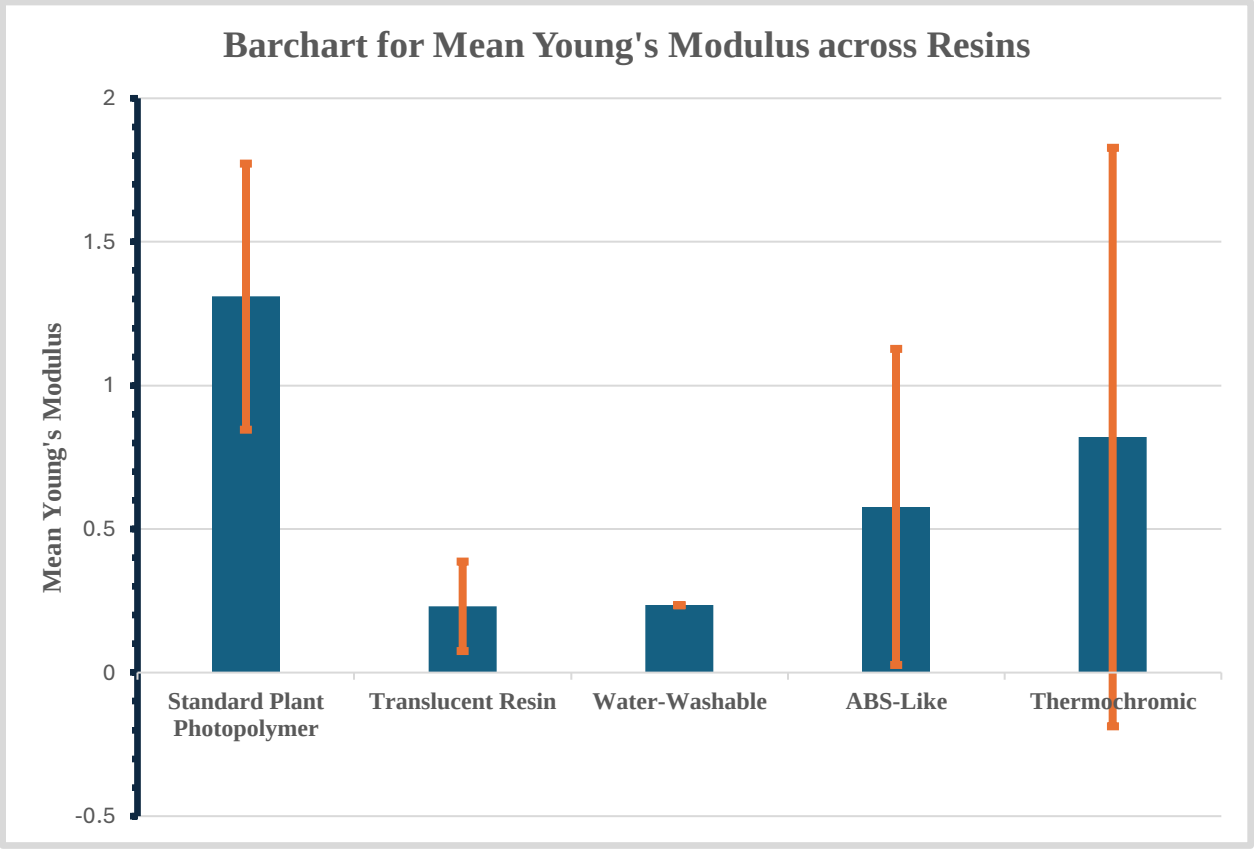

Fig. 3.3. 2 Young's Modulus of Elasticity For The Various Geometries

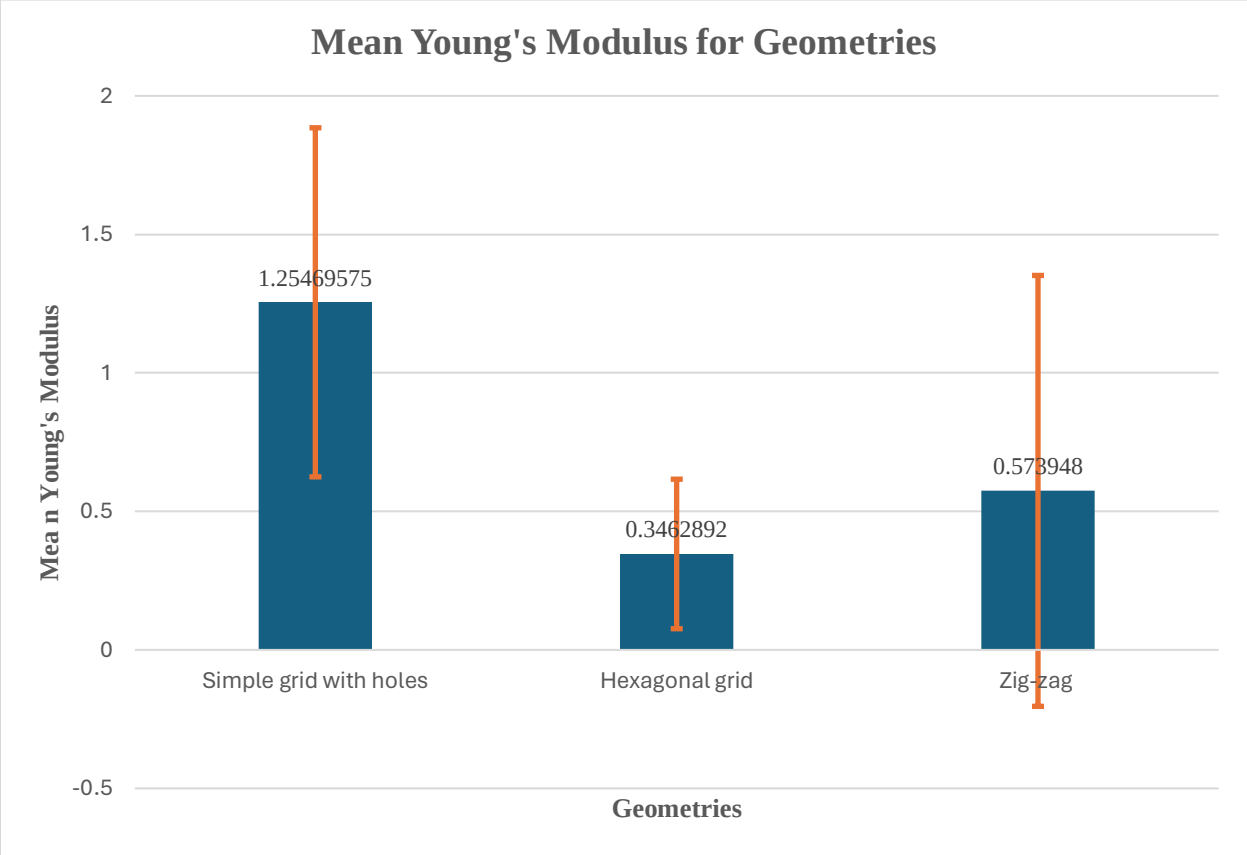

CHAPTER IV: DISCUSSION OF RESULTS

4.1 Print Times

From the results, time taken to print out designs was found to not only vary from geometry to geometry but also differs for the different types of printing materials used. The average time taken by the 3D printer to print a geometry was approximately 7.27 mins with a standard deviation of 1.97 mins. On average the translucent resin was the fastest to print for any geometry with an average of 5.47 mins whilst the thermochromic resin had the slowest print rate. Even though previous works did not record the print times, we deduced from this work that the time taken to print depended more on the type of printing material rather than the geometry with dimensions of designs the same throughout.

4.2 Printed Geometries

In designing the geometry prototypes, the same dimensions were used. However, print outs were found to have different thickness based on the type of resin used. Geometries printed with Translucent and ABS-like resins were found to be less thick than those from the other types of resin. This suggests that the type of material used in printing influences the thickness of geometries. This finding can also be due to fact that the different materials also required different slicing settings in Chitubox.

4.3 Mechanical Properties

In general, almost all the prototypes showed linear elastic activity up to a certain point and then began to break internally. All the plots beyond the linear elastic limit exhibited inconsistent rises and falls in stress activity until finally falling to a breaking strain point on the strain axis. Typically, plastic materials are expected to undergo some form of elastic deformation before finally breaking. In this work, the ultimate tensile strength represented by the highest stress point is not

solely the focus since we are not designing a material that is easily breakable. For a material to be both hard and flexible, there needs to be a gradual rise and peaking of the linear stress-strain plot.

Findings showed that the grid with holes geometry of the water washable resin (Fig. 3.2.14) required the highest force to break (Stress ≈ 6.555 N/mm²). However, it can be seen from the graph that there was no strain applied to the material before breaking, suggesting how brittle the material is (Strain = 0). The stress rose steeply on the vertical axis, demonstrating how hard it is to break the material. This result, compared to that of the same geometry printed with the other resins, showed that this material, even though tough in strength, cannot produce the best prototype when it comes to flexibility. This same finding can be seen with the zig-zag geometry of the water-washable resin (Fig. 3.2.16), even though it had a lower linear stress value. For this class of geometry, the ones printed with the translucent resin showed enough stretching before breaking (graph in Fig. 3.2.8). However, the ultimate stress was lower than expected for a material that had undergone so much strain. This suggests that even though this resin was able to improve the flexibility of the material, a lower force is required to break it. Also, the higher final breaking strain value seen can be attributed to the fact that the prototype underwent multiple internal breakages before finally breaking.

Results for the Zig-zag geometry showed similar traits as seen for the grid with holes geometry. Just like the grid with holes printed with water washable resin, the zigzag geometry from the same resin had a rapid rise in stress and quickly declined from the ultimate stress value to the breaking strain point (see fig. 3.2.16). However, unlike what was seen in the grid with holes, this geometry for water-washable resin had the lowest ultimate stress value (0.417 N/mm²) when compared to that of the same geometry for other resins. This suggests that this geometry is not only the least flexible but also the weakest in strength, an observation that is expected. The resin that demonstrated the ability to withstand the most strain before finally breaking for this group was again,

the translucent resin. This is shown in fig. 3.2.10 where the prototype, on average, went through several internal breaks after achieving a peak linear stress value before finally declining to a final breaking strain point of 72.986%. This result suggests the resin gave this material moderate or appreciable plastic abilities as compared to the same geometry for other resin types. One unusual observation was seen for this geometry for the ABS-like resin. A double peak in stress was seen (see Fig 3.2.12) suggesting that after the first linear phase of the plot before the first break in the prototype, the prototype required another higher stress to break internally after stretching a bit. This was witnessed in this geometry for the other types of resin as well. These sharp changes in the peak stress value from a declining point can be attributed to the wavy patterns seen between the grids. The idea to improve the flexibility of this type of geometry by incorporating wavy patterns into the design is similar to that of Li et al, 2019, where the same patterns were used to improve the stretchability with effective stiffness. This design enables the prototype to mimic the properties of collagen fibers, which also have wavy structures (Ushiki, 2002).

The hexagonal grid prototypes were the geometries that demonstrated the most typical plastic elasticity in their plots, especially for the Translucent resin (see Fig. 3.2.5). Although this geometry had an average peak stress (1.236 N/mm^2) across all resins when compared to the Simple grid with holes, the prototypes were able to demonstrate the linear phase and showed signs of going beyond the plastic limit before breaking. This result suggests, to some extent, that these prototypes have the highest possibility of returning to their original size after they are stretched. As seen for the previous geometries, the translucent resin type again proved to have improved the characteristics seen in this geometry. The water-washable resin, even though it had the highest peak stress value for this geometry, failed to have the above-stated characteristic and underwent several quick internal

breakages before hitting a final break strain value. This further confirms how brittle the prototypes printed with this material are.

The ASTM standard for testing plastic materials also uses the tensile modulus of elasticity to classify these materials based on their stiffness. The tensile modulus in this work was calculated by deducing the slope of the linear aspect of the stress-strain curve to represent the general formula for Elasticity, E as E = Stress/Strain. The results represented by the bar chart in Fig. 3.3 show the Simple grid with holes geometry to be the stiffest of all the geometries across all resin types with an average of ≈1.255 MPa, and the least stiff was the hexagonal grid geometry with an average of ≈0.346 MPa. These results suggest that, in general, the most flexible of the geometries is the hexagonal grid, and this result supports the observations seen in the previous results discussed above where the hexagonal grid pattern was seen to demonstrate plastic properties in its graph as compared to the other geometries. It was impossible to calculate the tensile modulus of elasticity for the grid with holes and zig-zag geometries for the water- washable resin because they only rose and declined on the stress axis without necessarily undergoing any form of strain. From Fig 3.3.2, the zig-zag geometry showed the second highest average tensile modulus. This observation suggests this geometry has some moderate level of both toughness and elasticity, an attribute that can be linked to the presence the wavy pattern designs in-between the simple grids. The same idea was adopted by Pattinson *et al* where they incorporated wavy designs in their geometry to allow stretchability until the material is taut. The findings stated so far are in line with some results obtained in previous works done. Results from this work, for instance, demonstrated that different geometries have an impact on the tensile and mechanical properties of prototypes, and this supports a similar finding by Fiadallah et al. in 2023 where they found tensile strength to be enhanced by rectangular shapes.

Across resins, the standard photopolymer resin showed the highest average toughness (≈1.309 MPa, see Fig. 3.2.1) whilst the translucent had the least toughness. The small average Young's modulus for the water-washable resin can be attributed to the fact that only the hexagonal grid under this resin with the other two geometries giving undefined results as explained in earlier paragraphs. The Translucent resin demonstrated the highest amount of flexibility and with the ABS-like following closely. Another observation from the elastic moduli calculation with reference to print speed (based on print time) was the translucent resin geometries having the least average elastic moduli and the lowest average print speed. This result is contrary to findings from a previous study by Bruère et al. in 2023 where they found higher print speed to result in lower elastic moduli. It is, however, assumed this difference in observation may be due to difference print method and materials used in the printing of prototypes.

In conclusion, the above observations show that in considering the geometry to go for in the future, I suggest focus is directed towards the zig-zag geometry. This geometry was able to demonstrate both strength and flexibility at a moderate level. Also, a look at the strength strain plot for this geometry showed the highest number of internal breakages before finally achieving a final break strain. This observation suggests the capability of this geometry to withstand fluctuations in impact forces when used in a knee brace, an attribute that can help in curbing the amount of final impact force the knee experiences. Notwithstanding the above stated, the selection of both materials and geometries in future works should depend more on the purposes and the type of mechanical property demands since different geometries and materials showed different mechanical properties.

CHAPTER V: SUMMARY AND FUTURE DIRECTIONS

The research was able to demonstrate the importance of considering both geometric design and resin (printing material) selection in 3D printing to achieve desired mechanical characteristics. While certain geometries may exhibit higher strength, they might also lack flexibility, as observed in prototypes printed with water washable resin. This study identifies the hexagonal grid geometry as demonstrating typical plastic elasticity, suggesting a higher potential for prototypes to return to their original shape after deformation. This finding supports the notion that geometric design plays a crucial role in determining mechanical behavior.

Secondly, the findings also show the differences inherent in material properties. For instance, while the translucent resin enhances flexibility, it tends to result in lower ultimate stress values compared to other resins. This indicates the need for a balanced approach to material selection based on specific application requirements.

Moreover, the analysis of tensile modulus of elasticity reveals variations across different geometries and resin types, emphasizing the intricate relationship between print parameters and material properties. Contrary to previous findings, the study observes that higher print speed does not necessarily result in lower elastic moduli, suggesting the influence of factors such as print method and material composition.

Overall, the research contributes to a deeper understanding of how geometric design and resin characteristics impact the mechanical performance of 3D-printed prototypes. By showing these relationships, this study provides valuable insights for optimizing material selection and geometric design to meet specific application needs, ultimately advancing the field of additive manufacturing.

Notwithstanding the above, this study however has some limitations due to time constraints and material and equipment availability. It is therefore a suggestion that future works should there focus on:

1. The use of better printing techniques such as extrusion methods which can explicitly program toolpath that can be used in additive manufacturing to produce finer prototypes.
2. Adding nanoparticles to printing materials to see how they affect the mechanical properties of the prototypes.
3. Incorporating synthetic fibers into printing process. This process does not only improve flexural rigidity and strength but also leaves the fiber unconstrained in areas of each unit cell, to only make it taut at critical strain where the highest stiffness is needed.

REFERENCES

1. Gross, B. C., Erkal, J. L., Lockwood, S. Y., Chen, C., & Spence, D. M. (2014). Analytical Chemistry, 86(7), 3240-3253. https://doi.org/10.1021/ac403397r

2. Li, J., Wu, C., Chu, P. K., & Gelinsky, M. (2020). 3D printing of hydrogels: Rational design strategies and emerging biomedical applications. In Materials Science and Engineering R: Reports (Vol. 140). Elsevier Ltd.

3. Pattinson, S. W., Huber, M. E., Kim, S., Lee, J., Grunsfeld, S., Roberts, R., Dreifus, G., Meier, C., Liu, L., Hogan, N., & Hart, A. J. (2019). Additive Manufacturing of Biomechanically Tailored Meshes for Compliant Wearable and Implantable Devices. Advanced Functional Materials, 29(32). https://doi.org/10.1002/adfm.201901815

4. Rengier, F., Mehndiratta, A., von Tengg-Kobligk, H., et al. (2010). 3D printing based on imaging data: review of medical applications. International Journal of Computer Assisted Radiology and Surgery, 5, 335–341. https://doi.org/10.1007/s11548-010-0476-x

5. Leukers, B., Gülkan, H., Irsen, S. H., et al. (2005). Hydroxyapatite scaffolds for bone tissue engineering made by 3D printing. Journal of Materials Science: Materials in Medicine, 16, 1121–1124. https://doi.org/10.1007/s10856-005-4716-5

6. Sing, S. L., An, J., Yeong, W. Y., & Wiria, F. E. (2016). Title of the article. Journal of Orthopaedic Research, 34, 369.

7. Martorelli, M., Gerbino, S., Giudice, M., & Ausiello, P. (2013). Dent. Mater., 29, e1.

8. Trombetta, R., Inzana, J. A., Schwarz, E. M., Kates, S. L., & Awad, H. A. (2017). Ann. Biomed. Eng., 45, 23.

9. He, Y., Xue, G., & Fu, J. (2015). Sci. Rep., 4, 6937.

10. Mondschein, R. J., Kanitkar, A., Williams, C. B., Verbridge, S. S., & Long, T. E. (2017). Biomaterials, 140, 170–188.

11. Biswas, M. C., Jony, B., Nandy, P. K., Chowdhury, R., Halder, S., Kumar, D., Ramakrishna, S., Hassan, M., Ahsan, A., Hoque, E., et al. (2022). Recent Advancement of Biopolymers and Their Potential Biomedical Applications. Journal of Polymers and the Environment, 30, 51–74.

12. Silbert, J. (2019, February 25). Nike finally launches vapor fly elite flyprint 3D, restricts sales to marathon runners. Hypebeast. https://hypebeast.com/2019/2/nike-vaporfly-elite-flyprint-3d-japan-release-info.

13. Nano Dimension. Title of the article. Retrieved from URL

14. Soe, S. P., Martin, P., Jones, M., Robinson, M., & Theobald, P. (2015). Feasibility of optimizing bicycle helmet design safety through the use of additive manufactured TPE cellular structures. International Journal of Advanced Manufacturing Technology, 79, 1975–1982.

15. Tensile Properties. (2014, February 16). Retrieved April 8, 2024, from [URL]

16. Ushiki, T. (2002). Collagen fibers, reticular fibers and elastic fibers: A comprehensive understanding from a morphological viewpoint. *Archives of Histology and Cytology, 65*(2), 109-126. doi:10.1679/aohc.65.109

17. Faidallah, R. F., Hanon, M. M., Vashist, V., Habib, A., Szakál, Z., & Oldal, I. (2023). Effect of different standard geometry shapes on the tensile properties of 3D-printed polymer. *Polymers (Basel), 15*(14), 3029. doi:10.3390/polym15143029

18. Bruère, V. M., Lion, A., Holtmannspötter, J., et al. (2023). The influence of printing parameters on the mechanical properties of 3D printed TPU-based elastomers. *Progress in Additive Manufacturing, 8*, 693–701. doi:10.1007/s40964-023-00418-